Pis'ma v ZhETF, vol. 84, iss. 8, pp. 514 – 518 © 2006 October 25

Exciton states in strongly coupled asymmetric semimagnetic double quantum dots

S. V. Zaitsev[1)], *M. K. Welsch*[+], *A. Forchel*[+], *G. Bacher*[*]

Institute of Solid State Physics RAS, 142432 Chernogolovka, Moscov reg., Russia

[+]*Technische Physik, Universität Würzburg, D-97074 Würzburg, Germany*

[*]*Lehrstuhl Werkstoffe der Elektrotechnik, Universität Duisburg-Essen, D-47057 Duisburg, Germany*

Submitted 5 September 2006

Exciton states in a pair of strongly coupled artificial asymmetric quantum dots (QDs) have been studied in magnetic field up to $B = 8\,\mathrm{T}$ by means of photoluminescence spectroscopy. The QD molecules have been fabricated by a selective interdiffusion technique applied to asymmetric CdTe/(Cd,Mg,Mn)Te double quantum wells. The lateral confinement potential within the plane, induced by the diffusion, gives rise to effective zero-dimensional exciton localization. Incorporation of the Mn ions in only one dot results in a pair of QDs with a markedly different spin splitting. In contrast to a positive value of the exciton Lande g-factor in nonmagnetic (Cd,Mg)Te-based single QDs, the ground exciton transition in the nonmagnetic QD demonstrates nearly zero g-factor, indicating a strong electron coupling between the dots. New low-energy band with a strong red shift appears at high B signifying formation of the indirect exciton, in accordance with our calculations.

PACS: 73.21.La, 75.50.Pp, 75.75.+a

Quantum dots (QDs) as zero-dimensional (0D) objects have attracted great interest during last years, because of the complete spatial carrier confinement results in a striking manifestation of reduced dimensionality effects [1]. Special interest to the double QDs with controllable interdot coupling has arisen with the development of the idea of quantum computing using spin degree of freedom as an information bit [2].

In the case of a single or double self-organized QDs with typical dot densities in the range of 10^9–10^{11} cm^{-2}, various optical techniques with high spatial resolution, such as micro-PL, near-field optical microscopy, metallic masks or etched mesas, have been developed in order to study individual dots [1]. In contrast to the epitaxial techniques, application of the nano-lithography for preparation of QDs allows the definition of individual dots with adjustable size. While straightforward access by the electron beam lithography and etching creates surface states at the open sidewalls which act as nonradiative centers, a promising way for realizing of the QDs makes use of a laterally selective intermixing between the quantum well (QW) layer and the barriers [3]. The selective interdiffusion causes a lateral change of the composition profile resulting in a QW bandgap E_g modulation and therefore in a lateral confinement of carriers. Single QDs have been realized by promoting the interdiffusion using a focused laser beam [4] or ion implantation followed by a rapid thermal annealing [3].

In this paper we present successful implementation of the novel approach for producing of the QD molecules with one nonmagnetic and another diluted magnetic semiconductor (DMS) QDs. Great advantage of the DMS heterostructures is that a giant Zeeman effect in such materials as CdMnTe makes possible continuous tuning of the E_g and exciton energies by external magnetic field, due to strong s,p-d exchange interaction between free carriers and localized d-states of Mn magnetic ions [5]. Effective g-factor of the DMS QD is strongly enhanced by incorporating of the Mn atoms allowing to vary the interdot coupling after preparation, when the structure parameters are fixed.

Starting asymmetric double QW was grown by molecular beam epitaxy on a thick CdTe buffer deposited on the (001)-oriented CdZnTe substrate. As grown structure has two nonmagnetic (NM) 6-nm wide CdTe QWs separated by a 3-nm wide $Cd_{0.8}Mg_{0.2}Te$ NM barrier. The outer NM $Cd_{0.8}Mg_{0.2}Te$ and the inner DMS $Cd_{0.8}Mn_{0.2}Te$ barriers are both 25-nm thick (Fig.1a).

To induce the lateral confinement of carriers, the selective interdiffusion technique was applied [6]. Basic idea behind the technique is depicted in Fig.1a. An upper 80 nm thick SiO_2 mask containing the apertures with diameters down to $D = 140\,\mathrm{nm}$ was defined by the electron beam lithography. Subsequently, the structure was annealed at a temperature 400 °C for 1 min., that in-

[1)]e-mail: zaitsev@issp.ac.ru

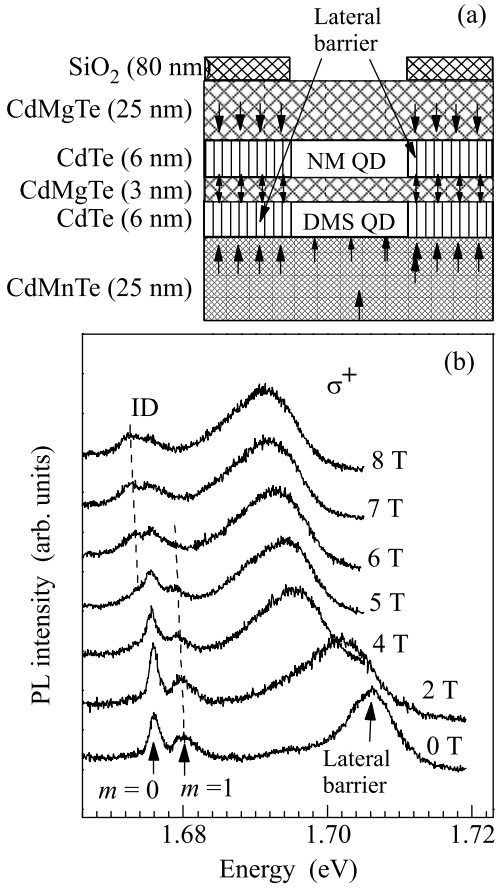

Fig.1. (a) A schematic illustration of the selective intermixing technique for fabrication of the asymmetric double QDs. Arrows indicate diffusion of the Mn and Mg atoms inside the QWs. (b) σ^+-polarized magneto-PL *cw* spectra of the double QDs with $D = 220$ nm in a Faraday geometry ($T = 1.5$ K). The spectra are shifted for clarity. Arrows denote the lateral barrier and NM QD exciton transitions with the angular quantum numbers $m = 0$ and $m = 1$. Dashed straight lines are to guide the eye

duces the interdiffusion between the QWs and barriers. As indicated by the arrows in Fig.1a, the interdiffusion is strongly enhanced below the mask as compared to non-covered areas and results in the increase of E_g below the masked areas, inducing a lateral confinement potential up to 0.3 eV and QD exciton levels' splitting up to 10 meV, depending on the sample and processing parameters [6]. In addition, bigger diffusion coefficient of the Mn as compared with the Mg [7] results in the diffusion of Mn atoms into the lower CdTe quantum well layer even within the apertures. Therefore, our approach results in a pair of the vertically aligned NM and DMS QDs where the incorporation of the Mn in the DMS QDs drastically enhances its effective g-factor [5]. Photoluminescence (PL) was measured in superfluid helium ($T = 1.5$ K) in a magnetic cryostat. Emission was excited by the continuous wave (*cw*) Ar^+ laser (line 514 nm) and recorded in Faraday geometry in two circular polarizations $\sigma^{\pm}$.

Fig.1b displays σ^+-polarized magneto-PL *cw* spectra of the double QDs with $D = 220$ nm. Two different kind of bands are observed at low B: a broad band at higher energy 1.706 eV, corresponding to the lateral barrier, and two narrow lines, ascribed to the NM QD intradot exciton transitions between an electron and a heavy hole (*hh*) states with angular quantum numbers $m = 0$ and $m = 1$ [8], similarly to the single NM QDs [6]. The high energy band, corresponding to the NM lateral barrier at low B, experiences strong red shift at $B > 1$ T in the σ^+ polarization while disappears in the σ^- polarization. Such kind of behavior, characteristic to the DMS QWs, is attributed to excitons in the DMS lateral barrier, which significantly lower energy with magnetic field due to the giant Zeeman effect. Note small linewidth of the $m = 0$ exciton transition (about 1.5 meV), which is reduced by a factor of 7 as compare to the 2D lateral barrier, a consequence of the effective 0D confinement and suppression of the inhomogeneous broadening in the QD.

In Fig.2a a magneto-PL behavior of the QD lines is shown with an enlarged scale. One can see that,

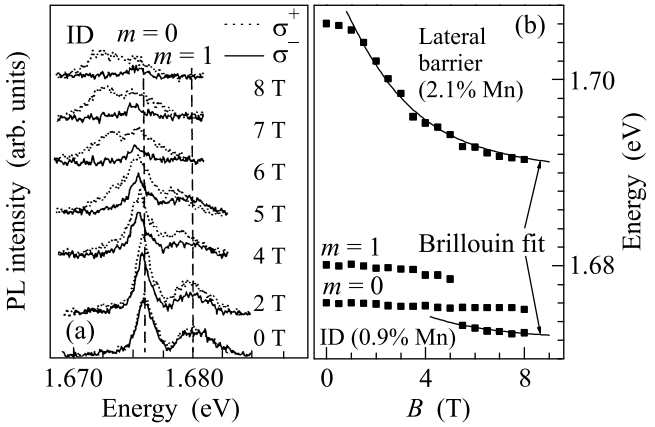

Fig.2. (a) Enlarged scale magneto-PL spectra of the double QDs with $D = 220$ nm (Fig.1b). The spectra are shifted for clarity. Dotted curves denote σ^+-polarization, solid – σ^--polarization. Dashed lines indicate zero field positions of the $m = 0$ and $m = 1$ transitions. (b) Magnetic field dependencies of exciton transitions in σ^+ polarization. Solid lines show results of the fit by the Brillouin function

in contrast to the positive exciton g-factor value in the NM CdMgTe-based QDs and expected diamagnetic blue shift [5], the ground $m = 0$ transition in both polarizations demonstrates slight red shift with increasing

B without noticeable Zeeman splitting. Simultaneously, strong reduction of the PL intensity is observed in σ^- polarization, which is characteristic to the DMS QDs [5]. The excited exciton state with $m = 1$ disappears at $B > 5$ T, also without evident Zeeman effect, while a new, σ^+-polarized low-energy band emerges at high B. It demonstrates strong red shift as compare to the NM intradot excitons and is ascribed to the indirect (ID) exciton state, according to our calculations. Absence of anticrossing behavior, observed recently in stress-induced QD molecules tuned by electric field [9], points to incoherent nature of the tunneling coupling in the studied structure. Strong elastic scattering via alloy fluctuations as a result of interdiffusion is assumed as the main coherence destruction mechanism. At the same time, intensity of the $m = 0$ exciton decreases at high B, pointing to a strong energy relaxation to the new state.

To understand the observed behavior in the investigated double QDs, numeric calculations of the exciton states have been performed. Calculations were done according to the adiabatic approximation [10], which separates carrier motion in the growth ($0z$) and radial (r) directions and is appropriate for QDs with big in-plane radius. Potential profiles of conductivity and valence bands in the $0z$ direction were approximated by a rectangular shape potential, which is a good approximation for deep QWs. The shape of the lateral potential $E_g(r)$ inside of the non-masked area was chosen as an error-function, which describes the in-plane diffusion [3]. Concentrations (atomic percentage) of the diffused Mn atoms in the DMS QD center and lateral barrier are evaluated by a fit with a modified Brillouin function [11] of the strong Zeeman shifts of the ID and DMS barrier excitons (Fig.2b) and amount to $\approx 0.9\%$ and 2.1%, respectively. The Mg contents at the center of both QDs and lateral barriers are estimated by a fit of the calculated transition energies to the experimental ones at $B = 0$ T and are found to be $\approx 1.4\%$ and 3.1% for the NM QD and 0.8% and 1.6% in the DMS QD, correspondingly.

Figure 3a shows z-components of the electron and hh wave functions in the center of the QDs at zero and high B. At $B = 0$ T both electron and hh-states, mainly localized in the DMS QD ($e2$ and $h2$), are higher in energy than those in the NM QD ($e1$ and $h1$). One can see that the hh-states are strongly localized in adjacent QDs. Contrary, electrons demonstrate strong tunnel coupling. At $B > 0$ the giant Zeeman effect in the DMS barrier and QD dramatically decreases band energies for states, corresponding to the σ^+-polarized transition, with the main change in the valence band, as the exchange constant is much stronger for the hh-states [11]. The hh levels cross at $B \approx 1.5$ T while electron levels never cross, according to the calculations.

Direct and ID exciton binding energies E_X are calculated using 2D approach [12], which is valid for strongly coupled QWs and is supposed to be approximate for the studied QD with large lateral extensions (exceeding bulk exciton Bohr radius). E_X is evaluated to be 14 ± 0.5 meV for both direct excitons and 10 ± 0.5 meV for both ID excitons in the whole magnetic field range, despite of the strong band shifts due to the giant Zeeman effect in the DMS QD. Large value of E_X for the ID excitons reflects the strong electron coupling between the QDs.

Figure 3b summarizes the calculated magnetic field dependencies of the 1st and 2nd electron ($e1$,$e2$) and hh ($h1, h2$) single-particle state energies with different spins projections, according to usual notation [11]. Note that the Lande band g-factors are not accounted for in these calculations. Obtained from such calculations energy levels for normal-to-plane motion with r-dependent energies were then treated as an effective potential for the radial motion, accordingly to the adiabatic approach [10]. The calculated in this way magnetic field dependencies of four possible exciton transitions between $m = 0$ states and which account for all contributions: the giant Zeeman band shift and the Lande band g-factors, are presented in Fig.3c. The exciton Lande g-factor of ≈ 2.14, which was found in the same width single NM QD, is used in the calculations. Two exciton states ($e1$-$h1$ and $e2$-$h2$) are the direct ones, while another two – indirect. The $e1$-$h1$ and $e1$-$h2$ states correspond to the observed in the experiment $m = 0$ and ID transitions, respectively. One can see that the ID exciton $e1$-$h2$ is the ground state at high B. It is a strong tunnel coupling between the QDs that gives rise to large value of E_X for the ID exciton $e1$-$h2$ (≈ 10 meV), comparable with that for the direct $e2$-$h2$ exciton in the DMS QD (≈ 14 meV), which is responsible for ground state of the ID at high B (Fig.3c). Rather broad ID band has linewidth of about two times bigger than that of the $m = 0$ transition, which is typical for indirect excitons and opposite to the direct excitons in the DMS QDs [13]. This fact also confirms our conclusion about indirect origin of the ID band.

Note that the $m = 1$ transition also corresponds to the $e1$-$h1$ exciton state but with the angular quantum number $m = 1$ of the radial component of full wave function. The calculated lateral potential profiles and radial components of the electron and hh single-particle wave functions, mainly localized in the NM QD and DMS QD, correspondingly, are presented in Fig.4 for $B = 0$ T and 8 T. The strong electron tunnel coupling between QDs provides an effective energy relaxation of the direct $e2$-$h2$ exciton in the DMS QD to the $e1$-$h1$

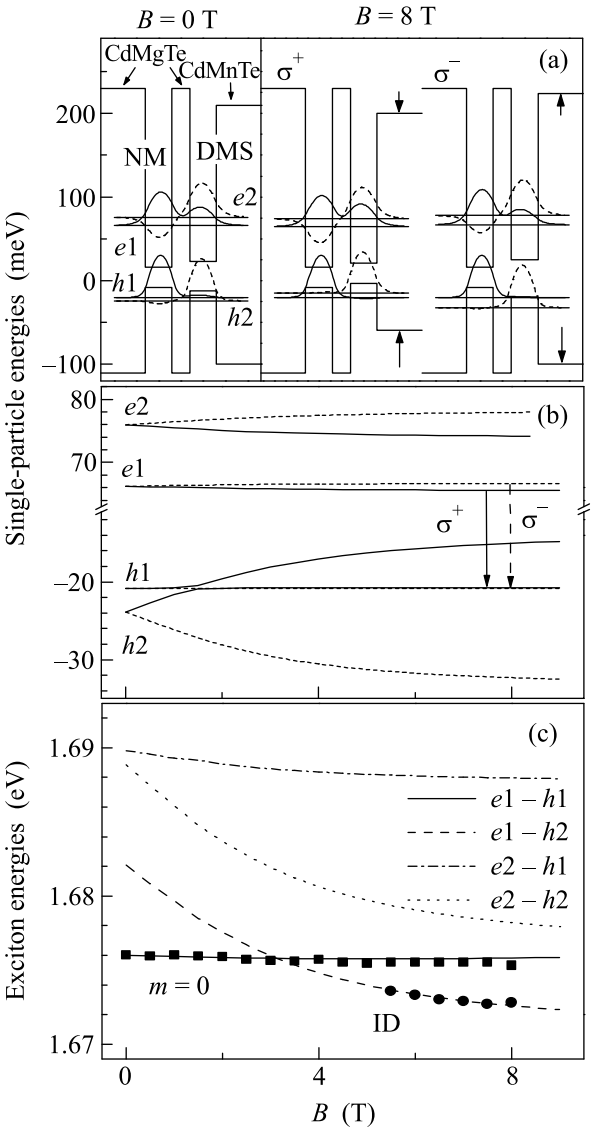

Fig.3. Results of the calculations: (a) normal-to-plane band profiles in the QD center for electron ($S_z = -1/2$) and heavy-hole ($J_z = -3/2$) states (σ^+ label) and ones with $S_z = +1/2$ and $J_z = +3/2$ (σ^- label) at $B = 0$ T and 8 T. Carrier states are denoted according to the usual notation [11]. Energy scale is offset to the band edges of a bulk CdTe. Normal-to-plane wave function components in the NM QD (solid line) and DMS QD (dashed line) are shifted according to the level energy. Arrows show direction of the band movement with magnetic field; (b) the magnetic field dependencies of the electron ($e1, e2$) and heavy hole ($h1, h2$) single-particle state energies. The Lande band g-factors are not accounted for in this calculations. Solid lines mark the states corresponding to σ^+-polarized optical transitions, dashed lines – for σ^--polarized transitions; (c) the calculated dependencies of σ^+-polarized exciton transitions (lines) and experimental values (symbols) with accounting for all contributions

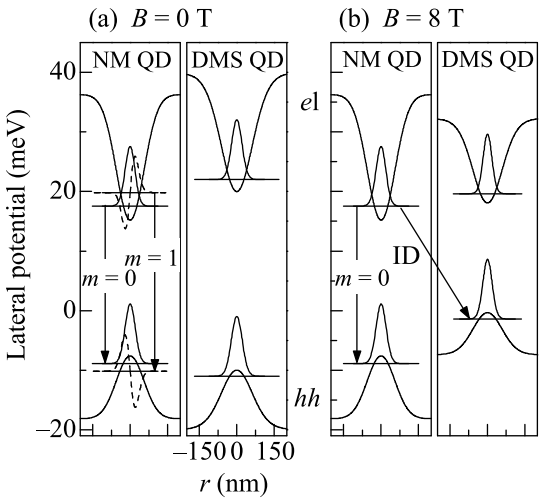

Fig.4. Calculated lateral band potential profiles, electron (el) and heavy hole (hh) radial wave functions and for states with $m = 0, 1$ quantum numbers (solid and dashed lines, respectively) for QD molecule with $D = 220$ nm at (a) $B = 0$ T and (b) $B = 8$ T. Arrows show corresponding direct and ID exciton transitions. Energy scale is offset relatively to the energy levels in a single 6 nm wide CdTe QW

state in the NM QD at low B and to the $e1$-$h2$ ID state at high B. This explains the absence of the exciton emission from the DMS QD in the PL spectra. By the same reason the $m = 0$ and $m = 1$ excitons effectively relax to the ID state at high B when the ID transition is the lowest one in energy.

In a finite magnetic field the energy sequence of exciton states, corresponding to the σ^+- and σ^--polarized optical transitions, is opposite in the NM and DMS CdTe-based QDs. In the DMS QDs, the splitting of electron and hole states is provided by the strong *sp-d* exchange interaction with localized Mn^{2+} ions [11]. That results in a huge negative g_{hh} and positive g_e effective g-factors of the hh and electron states, respectively, and σ^+-polarization of the ground exciton transition in the CdMnTe at $B > 0$. Contrary, in the NM CdMgTe-based QDs the g_{hh} is small and positive, while g_e is negative [5, 14]. As a result, the lowest bright exciton state is σ^--polarized.

According to the calculations (Fig.3b), it is a strong electron tunnel coupling between the NM and DMS QDs which is responsible for a positive contribution to the g_e and gives rise to the unusual electron levels' splitting in the NM QD. Thus, in the studied double QD system we attribute spectrally unresolved coincidence of the σ^+ and σ^--polarized components of the $m = 0$ transition to a nearly compensation of the two factors: a Zeeman splitting due to the Lande band g-factor, which amounts $\approx$1 meV at $B = 10$ T in both NM CdMgTe QWs and

QDs [5, 14], and an opposite splitting of the delocalized electron ground level e1 due to the giant Zeeman effect in the DMS QD. The observed total slight red shift of the m=0 exciton also evidences about strong tunnel coupling between the NM and DMS QDs realized in the studied double QDs, as confirmed by our calculations.

Level splitting between the $m = 0$ and $m = 1$ transitions amounts 4 meV at $B = 0$ T. It is considerably smaller than the direct exciton binding energy of 14 meV, pointing to a weak exciton confinement regime [15]. Calculations of the radial part of Schrodinger equation show that this value of splitting requires effective QD diameter $D \simeq 100$ nm. It is smaller than the nominal QD diameter and evidences about strong in-plane diffusion. Lateral extensions of the calculated ground electron- and hh-wave functions are significantly smaller, of about 18 nm (Fig.4), a consequence of error-function shape of the lateral confining potential, but exceed exciton Bohr radius, confirming weak confinement regime of excitons in the studied QDs.

To summarize, we presented a novel approach for realization of the asymmetric QD molecules in which the effective g-factors of both nonmagnetic and semimagnetic dots are strongly influenced by incorporating of the magnetic ions. It is found that the tunnel coupling in the double QD system with a narrow barrier can be so strong that results in a significant change of the electron g-factor in the nonmagnetic QD and, also, in the formation of the indirect exciton between the electron of the nonmagnetic QD and heavy hole of the DMS QD at high magnetic field.

This work is supported by Russian Foundation for Basic Research, grants # 04-02-17338 and # 06-02-17404.

1. N. N. Ledentsov, V. M. Ustinov, V. A. Shchukin et al., Semiconductors **32**, 343 (1998).
2. D. D. Awschalom, D. Loss, and N. Samarth, *Semiconductor spintronics and quantum computation*, Springer series: NanoScience and Technology, Springer-Verlag, 2002.
3. G. Bacher, T. Kümmell, D. Eisert et al., Appl. Phys. Lett. **75**, 956 (1999).
4. K. Brunner, U. Bockelmann, G. Abstreiter et al., Phys. Rev. Lett. **69**, 3216 (1992).
5. G. Bacher, H. Schömig, J. Seufert et al., Phys. Stat. Sol. (b) **229**, 415 (2002).
6. S. V. Zaitsev, M. K. Welsch, H. Schömig et al., Semicond. Sci. Technol. **16**, 631 (2001).
7. D. Tönnies, G. Bacher, A. Forchel et al., J. Cryst. Growth **138**, 362 (1994).
8. U. Bockelmann, Phys. Rev. B **50**, 17271 (1994).
9. H. J. Krenner, M. Sabathil, E. C. Clark et al., Phys. Rev. Lett. **94**, 057402 (2005).
10. M. Korkusinski and P. Hawrylak, Phys. Rev. B **63**, 195311 (2001).
11. D. R. Yakovlev and K. V. Kavokin, Comments Condens. Matter Phys. **18**, 51 (1996).
12. R. P. Leavitt and J. W. Little, Phys. Rev. B **42**, 11774 (1990).
13. G. Bacher, A. A. Maksimov, H. Schömig et al., Phys. Rev. Lett. **89**, 127201 (2002).
14. A. A. Sirenko, T. Ruf, M. Cardona et al., Phys. Rev. B **56**, 2114 (1997).
15. T. Takagahara, Phys. Rev. B **47**, 4569 (1993).